Cyclin D1 and CDK4 Activity Contribute to the Undifferentiated Phenotype in Neuroblastoma

Jan J. Molenaar,[1] Marli E. Ebus,[1] Jan Koster,[1] Peter van Sluis,[1] Carel J.M. van Noesel,[3] Rogier Versteeg,[1] and Huib N. Caron[2]

[1]Departments of Human Genetics and [2]Pediatric Oncology, Emma Kinderziekenhuis, and [3]Department of Pathology, Academic Medical Center, University of Amsterdam, Amsterdam, the Netherlands

Abstract

Genomic aberrations of Cyclin D1 (CCND1), CDK4, and CDK6 in neuroblastoma indicate that dysregulation of the G_1 entry checkpoint is an important cell cycle aberration in this pediatric tumor. Here, we report that analysis of Affymetrix expression data of primary neuroblastic tumors shows an extensive overexpression of Cyclin D1, which correlates with histologic subgroups. Immunohistochemical analysis showed overexpression of Cyclin D1 in neuroblasts and low Cyclin D1 expression in all cell types in ganglioneuroma. This suggests an involvement of G_1-regulating genes in neuronal differentiation processes which we further evaluated using RNA interference against Cyclin D1 and its kinase partners CDK4 and CDK6 in several neuroblastoma cell lines. The Cyclin D1 and CDK4 knockdown resulted in pRb pathway inhibition as shown by an almost complete disappearance of CDK4/CDK6-specific pRb phosphorylation, reduction of E2F transcriptional activity, and a decrease of Cyclin A protein levels. Phenotype analysis showed a significant reduction in cell proliferation, a G_1-specific cell cycle arrest, and, moreover, an extensive neuronal differentiation. Affymetrix microarray profiling of small interfering RNA–treated cells revealed a shift in expression profile toward a neuronal phenotype. Several new potential downstream players are identified. We conclude that neuroblastoma functionally depend on overexpression of G_1-regulating genes to maintain their undifferentiated phenotype. [Cancer Res 2008;68(8):2599–609]

Introduction

Neuroblastic tumors develop from progenitor cell types that originate from the neural crest. These tumors are classified into neuroblastoma and the more differentiated counter parts, ganglioneuroblastoma and ganglioneuroma. This histopathologic classification is based on morphologic features of the tumor. Undifferentiated neuroblastoma at one end of the spectrum contain mainly neuroblasts, whereas on the other end, ganglioneuroma consist of ganglion cells, Schwann cells, and stroma cells (1, 2). This spectrum of neuroblastic tumors is reflected in the development of nonmalignant neuroblasts that differentiate along neural crest cell lineages to neuronal ganglia and chromaffin cells (3–5). The Schwann cells in neuroblastic tumors are believed to be normal cells invading the tumor and not to originate from the malignant neuroblasts, although some researchers have disputed this (6–8). The molecular mechanism underlying the differentiation pattern and the differences between these neuroblastic tumor types have been subject of several studies. Growth signaling pathways and specific neurotrophins and their receptors have been found to determine differentiation patterns in nonmalignant neuroblasts and influence the differentiation state of neuroblastoma (9–11).

Recently, some papers functionally link neuronal differentiation to cell cycle regulation, which frequently involves the G_1 cell cycle entry point (12–15). This is a tightly controlled process by the D-type cyclins and their kinase partners CDK4 and CDK6. In the presence of cyclin D, these kinases phosphorylate the pRb protein, which then releases from the E2F transcription factor. Subsequent transcription of key regulator genes allows further progression of the cell cycle (16). In neuroblastic tumors, several oncogenetic events causing changes in cell cycle regulation have been described. Amplifications of CDK4 and one mutation in CDK6 that disrupts p16 binding have been identified (17–19). We have reported amplification of the Cyclin D1 gene in 5 of 203 neuroblastic tumors and a rearrangement in the 3′ untranslated region of the Cyclin D1 gene in one tumor (20). The sporadic genomic aberrations of CDK4, CDK6, and Cyclin D1, together with the findings of the very high Cyclin D1 expression levels, suggested that dysregulation of the G_1 entry checkpoint is an important cell cycle aberration in neuroblastoma.

In this paper, a detailed analysis of Cyclin D1 overexpression by Affymetrix profiling and immunohistochemical analysis of neuroblastic tumors reveals that the overexpression is specific for malignant neuroblasts. We show that silencing of Cyclin D1 and its kinase partner CDK4 causes an inhibition of the cyclin D1-pRb pathway, a G_1 cell cycle arrest and growth arrest. Moreover, we show a clear differentiation toward a neuronal cell type by immunofluoresence and Affymetrix Microarray analysis after Cyclin D1 and CDK4 silencing.

Materials and Methods

Patient samples. The neuroblastic tumor panel used for Affymetrix microarray analysis contains 88 neuroblastoma samples, 11 ganglioneuroblastoma samples, and 11 ganglioneuroma samples. All samples were derived from primary tumors of untreated patients. Material was obtained during surgery and immediately frozen in liquid nitrogen. N-Myc amplifications and 1p deletions were all determined using Southern blot analysis of tumor material and lymphocytes of the same patient.

Cell lines. Cell lines were cultured in DMEM supplemented with 10% fetal bovine serum, 20 mmol/L L-glutamine, 10 units/mL penicillin, and 10 μg/mL streptomycin. Cells were maintained at 37°C under 5% CO_2. For primary references of these cell lines, see Cheng et al. (21).

RNA isolation, Northern blotting, and Affymetrix microarray analysis. Total RNA of neuroblastoma tumors was extracted using Trizol reagent (Invitrogen) according to the manufacturer's protocol. RNA concentration was determined using the NanoDrop ND-1000, and quality

Requests for reprints: Jan J. Molenaar, Department of Human Genetics, AMC, M1-132, Meibergdreef 15, 1105 AZ Amsterdam, the Netherlands. Phone: 31-20-5667536; Fax: 31-20-6918626; E-mail: j.j.molenaar@amc.uva.nl.

doi:10.1158/0008-5472.CAN-07-5032

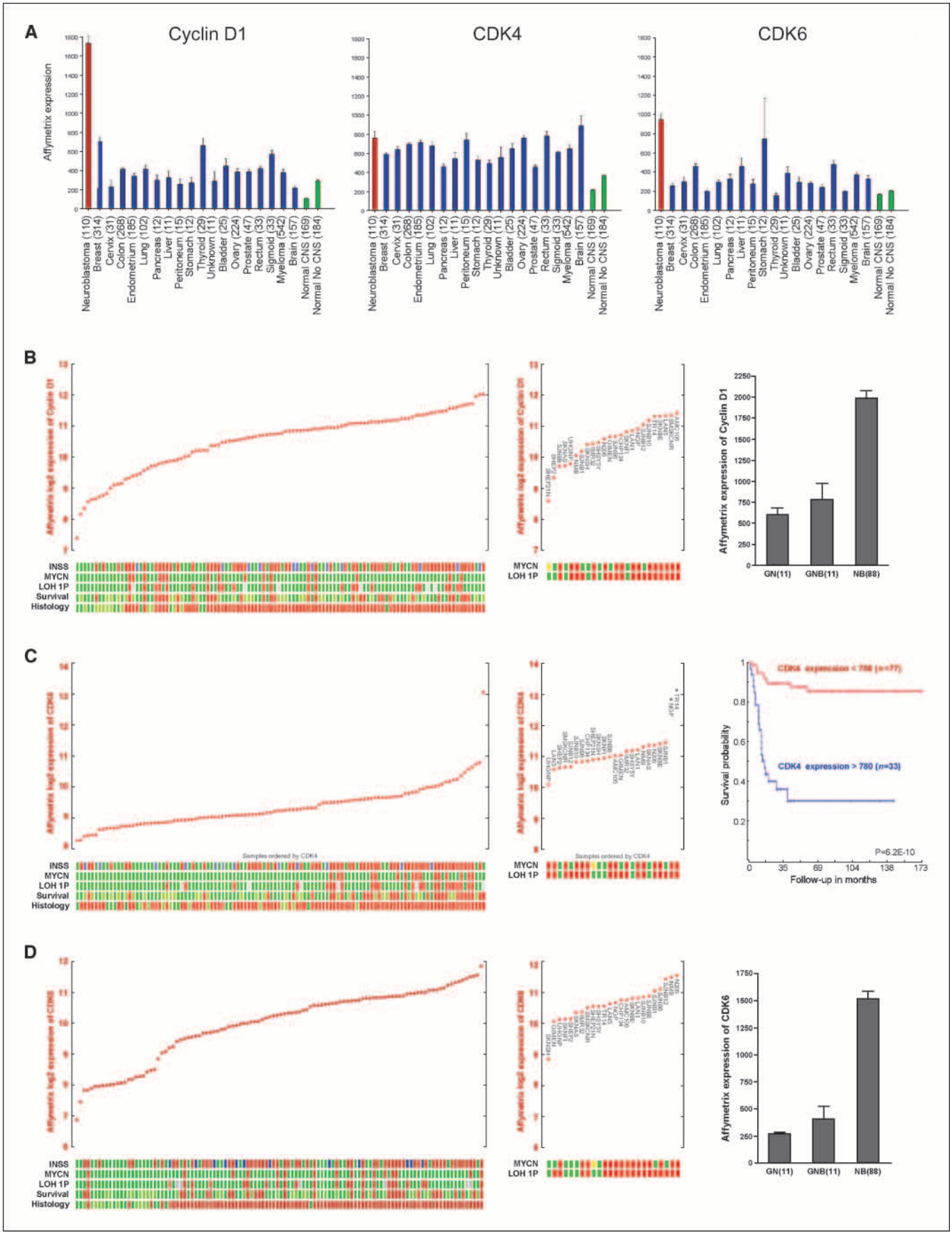

was determined using the RNA 6000 Nano assay on the Agilent 2100 Bioanalyzer (Agilent Technologies). For Northern blotting, 15 μg of RNA were electrophoresed through a 1% agarose gel containing 6.7% formaldehyde and blotted on Hybond N membrane (Amersham) in 16.9 × SSC and 5.7% formaldehyde. The Cyclin D1 probe was generated by reverse transcription–PCR. We used the following primers: 5′-tcattgaacactcctctcc-3′ and 5′-gtcacacttgatcactctgg-3′. Probes were sequence verified. Probes were ^{32}P labeled by random priming. We hybridized Northern blot filters for 16 h at 65°C in 0.5 mol/L Na_2HPO_4, 7% SDS, 1 mmol/L EDTA, and 50 μg/mL herring sperm DNA. Measurement of signal intensity was performed with a Fuji phosphor imager and Aida 2.41 software. Affymetrix microarray analysis, fragmentation of RNA, labeling, hybridization to HG-U133 Plus 2.0 microarrays, and scanning were carried out according to the manufacturer's protocol (Affymetrix, Inc.). The expression data were normalized with the MAS5.0 algorithm within the GCOS program of Affymetrix. Target intensity was set to 100 ($\alpha1 = 0.04$ and $\alpha2 = 0.06$). If more then one probe set was available for one gene, the probe set with the highest expression was selected, considered that the probe set was correctly located on the gene of interest. Public available Affymetrix expression data was taken from the National Cancer Institute (NCI) Gene Expression Omnibus database.[4]

Immunohistochemistry. Paraffin-embedded tumors were cut into 4-μm sections, mounted on aminoalkylsaline-coated glass slides, and dried overnight at 37°C. Sections were dewaxed in xylene and graded ethanol, after which they were fixed, and endogenous peroxidase was blocked in a 0.3% H_2O_2 solution in 100% methanol. Subsequently, the slides were rinsed thoroughly in distilled water and incubated in a 0.01 mol/L sodium citrate solution (pH 7.1) in an autoclave. After 10 min at 120°C, the sections were left to cool for at least 5 min. After rinsing in distilled water and PBS, the last step in pretreatment is 10-min incubation in a normal goat serum solution (10% in PBS). For detection of Cyclin D1, we used a mouse monoclonal DCS-6 (Neomarkers) as a primary antibody. Slides were incubated overnight at 4°C in a 1:1,000 dilution in a solution of 1% bovine serum albumin (BSA) in PBS (1% PBSA). Slides were then blocked with a postantibody blocking (Power Vision kit, ImmunoLogic) 1:1 diluted in PBS for 15 min, followed by a 30-min incubation with poly–horseradish peroxidase (HRP)–goat α mouse/rabbit IgG (Power Vision kit, ImmunoLogic) 1:1 diluted in PBS. Chromogen and substrate were 3,3′-diaminobenzidine (DAB) and peroxide (1% DAB and 1% peroxide in distilled water). A 2-min incubation time results in a brown precipitate in Cyclin D1–positive nuclei. Nuclear counterstaining was done with hematoxylin. After dewatering in graded ethanol and xylene, slides were coated with glass and evaluated independently by two observers. As a positive control, mantle cell lymphomas were used, and as negative controls, two Burkitt lymphoma samples were used.

RNA interference. The small interfering RNA (siRNA) oligonucleotides were synthesized by Eurogentec. Three different siRNAs were designed, targeting Cyclin D1 on nucleotides 855 to 875 (CD1-A), 345 to 365 (CD1-B), and 671 to 691 (CD1-C) according to Genbank accession NM_053056. The CDK4 siRNA is targeting nucleotides 1062 to 1082 according to Genbank accession NM_000075. The CDK6 siRNA is targeting nucleotides 1112 to 1132 according to Genbank accession NM_001259. A previously designed siRNA directed against green fluorescent protein (GFP) was used as negative control (sense sequence: GACCCGCGCCGAGGUGAAGTT). Neuroblastoma cell lines were cultured for 24 h in 6-cm plates and transfected with 5.5 μg siRNA using Lipofectamine according to manufacturers' protocol.

Transactivation assays. The following luciferase constructs were used in the transactivation assays: pGL3 TATAbasic-6xE2F (pGL3 containing a TATA box and six E2F binding sites was previous tested for E2F selectivity and was a kind gift of Prof. R. Bernards, Dutch Cancer Institute; ref. 22), Renilla luciferase vector under cytomegalovirus promoter (pRL-CMV). Cells were cultured for 24 h in six-well plates, and transfections were conducted using Lipofectamine 2000 according to manufacturers' protocol. pGL3TA-TAbasic-6xE2F (0.8 μg) vector was transfected, together with the 0.8 μg pRL-CMV vector and Cyclin D1 siRNA or GFP siRNA. Dual-luciferase assays were performed after 48 h using the Promega dual-luciferase reporter assay system. For each assay, three separate experiments were performed.

Western blotting. The neuroblastoma cell lines were harvested on ice and washed twice with PBS. Cells were lysated in a 20% glycerol, 4% SDS, 100 mmol/L Tris-HCl (pH 6.8) buffer. Protein was quantified with RC-DC protein assay (Bio-Rad). Loading was controlled by Bio-Rad Coomassie staining of a reference SDS-PAGE gel. Lysates were separated on a 10% or 5% SDS-PAGE gel and electroblotted on a transfer membrane (Millipore). Blocking and incubation were performed using standard procedures. DCS-6 mouse monoclonal Cyclin D1 (Neomarkers), CDK4 C22 rabbit polyclonal (Santa Cruz), CDK6 C21 rabbit polyclonal (Santa Cruz), pRb Ser^{780} rabbit polyclonal (Cell Signaling Technology), Cyclin A clone 25 mouse monoclonal (Novocastra), actin C2 mouse monoclonal (Santa Cruz), and tubulin (Boehringer) antibodies were used as primary antibodies. After incubation with a secondary sheep anti-mouse or anti-rabbit HRP-linked antibody (Amersham), proteins were visualized using an enhanced chemiluminescence detection kit (Amersham). Antibodies were stripped from the membrane using a 2% SDS, 100 mmol/L β-mercapto-ethanol, 62.5 mmol/L Tris-HCl (pH 6.7) buffer.

Cell counting. All cell counting experiments were performed in duplo. Cells were collected by trypsinization and diluted in 1 mL of medium. Two samples of 100 μL of this medium were diluted in 100 μL Triton X-100/sapponine and 10 mL isotone II, and duplo counting of these two samples was performed on a Beckman Coulter Counter.

Fluorescence-activated cell sorting analysis. Cells were grown for 24 h in 12-well plates and then transfected with siRNA as described before. At 48 or 72 h after transfection, cells were lysated in the wells with a 3.4 mmol/L trisodiumcitrate, 0.1% Triton X-100 solution containing 50 μg/μL propidium iodide. After 1-h incubation, DNA content of the nuclei was analyzed using a fluorescence-activated cell sorter. A total of 30,000 nuclei per sample was counted. The cell cycle distribution and apoptotic sub-G_1 fraction was determined using WinMDI version 2.8.

TUNEL assay. Apoptotic cells were detected using the *in situ* cell death detection kit from Roche applied science. Cells with green fluorescent nuclei were indicated as apoptotic cells. The apoptosis index was the

[4] GSE2109 (https://expo.intgen.org/expo/public/listPublicGeoTransactions.do), GSE4290 (http://rembrandt-db.nci.nih.gov), GSE2658 (http://lambertlab.uams.edu).

Figure 1. Expression analysis of G_1 phase–regulating cyclins and cyclin-dependent kinases in neuroblastoma. *A,* the average Affymetrix microarray mRNA expression levels of Cyclin D1, CDK4, and CDK6 in various adult tumor types (*blue*) and normal tissues samples (*green*) compared with neuroblastic tumors samples (*red*). The number in brackets for each tumor tissue type indicates the number of samples. *Error bars,* SE. The source for the public available data is given in Materials and Methods. *B,* Affymetrix microarray expression of Cyclin D1 (log2-transformed) in individual neuroblastic tumor samples ($n = 110$) and neuroblastoma cell lines ($n = 24$), ordered by the log2-fold–transformed level of Cyclin D1 expression. For each tumor sample and each cell line, several characteristics are given as tracks (color-coded boxes). INSS: *red,* stages 3 or 4; *green,* stages 1 or 2; *blue,* Stage 4S. MYCN: *green,* nonamplified; *red,* amplification >10 copies; *orange,* contains MYCN expression vector. LOH1p: *red,* LOH1p; *green,* no LOH1p; *gray,* noninformative. Survival: *red,* death; *light green,* survival = 0 -5 y; *dark green,* survival >5 y. Histology: *red,* neuroblastoma; *dark green,* ganglioneuroblastoma; *light green,* ganglioneuroma. The bar plot shows the average Affymetrix microarray expression of Cyclin D1 in ganglioneuroma (*GN*), ganglioneuroblastoma (*GNB*), and neuroblastoma (*NB*). *C,* affymetrix microarray expression of CDK4 (log2-transformed) in individual neuroblastic tumor samples ($n = 110$) and neuroblastoma cell lines ($n = 24$) ordered by the level of CDK4 expression. Further information is as in *B*. The Kaplan-Meier curve shows the survival of patients with CDK4 Affymetrix microarray expression above 780 ($n = 33$) compared with below 780 ($n = 77$). *D,* Affymetrix microarray expression of CDK6 (log2-transformed) in individual neuroblastic tumor samples ($n = 110$) and neuroblastoma cell lines ($n = 24$) ordered by the level of CDK6 expression. Further information is as in *B*. The bar plot shows the average Affymetrix microarray expression of CDK6 in ganglioneuroma, ganglioneuroblastoma, and neuroblastoma.

Table 1. Results of immunohistochemical staining of 97 neuroblastic tumors containing 8 ganglioneuroma, 26 ganglioneuroblastoma, and 63 neuroblastoma

Tumor type	Cyclin D1 immunohistochemistry				
	−	+	++	Focal +	Total
Ganglioneuroma	7	1	0	0	8
Ganglioneuroblastoma	10	5	3	8	26
Neuroblastoma	6	30	23	4	63
Total	23	36	26	12	97

NOTE: Tissue was considered positive if at least 10% of the tumor cells showed specific nuclear staining, strongly positive when in at least 20% of the stained nuclei the hematoxylin counterstain was not visible any more, and focal-positive when only a part of the tumor showed nuclear staining.

number of apoptotic cells divided by the total number of cells. For each experiment, 500 cells were counted.

Fluorescence microscopy. Cells were grown on glass and transfected as described above. Cells were rinsed twice with PBS and fixed on glass using 4% paraformaldehide in PBS for 30 min. One more wash step was performed using PBS permeabilization of the cells using 0.05% Triton X-100 in PBS. After three more wash steps using 0.01% Triton X-100 in PBS, slides were blocked in 1% BSA, 0.01%Triton X-100, and PBS. This was followed by 15-min incubation with 0.1 μg phalloidin-TRITC labeled (Sigma-Aldrich) in 100 μL blocking solution. Slides were washed four times with 0.01% Triton X-100 in PBS and finally with H_2O. After drying, slides were mounted in Vectashield with 25 μg/mL propidium iodide.

Results

Expression of G_1 phase–regulating cyclins and cyclin-dependent kinases. Affymetrix expression profiles of 110 neuroblastic tumors allowed us to analyze expression levels of G_1-regulating genes *in vivo*. First we compared our data with publicly available Affymetrix HG-U133-plus2 expression profiles of 353 normal samples and 2,047 tumor samples (see Materials and Methods for references). Of the G_1-regulating cyclins, the Cyclin D1 gene shows the most abundant expression (Fig. 1*A*). The average Cyclin D1 expression in neuroblastic tumors is six times higher compared with normal tissue (n = 184) and 16 times higher compared with normal central nervous system tissue series (n = 169). Also, compared with libraries of 18 common malignancies, the Cyclin D1 expression in neuroblastoma is 2.5-fold to 7.5-fold higher. Even tumor types with known high frequency of genetic aberrations of the Cyclin D1 11q13 locus, such as breast tumors and myeloma, have lower expression of Cyclin D1 compared with neuroblastoma. The partners of Cyclin D1, the G_1-regulating CDK4 and CDK6, show interesting expression patterns. CDK4 and CDK6 are both highly expressed in neuroblastoma compared with various normal tissues, and the CDK4 expression level is comparable with adult tumors. To further analyze the expression of Cyclin D1, CDK4, and CDK6 in neuroblastoma, we generated plots of neuroblastic tumors and cell lines. Figure 1*B* shows that the Cyclin D1 expression (log2 values shown) in cell lines is within range of the *in vivo* expression. In our neuroblastoma series, we could identify a weak correlation between Cyclin D1 expression levels and INSS tumor stage and a very significant correlation with the histologic classification of neuroblastic tumors (ganglioneuroma versus neuroblastoma unpaired Student's t test, $P = 1.2 \times 10^{-13}$). The plot of CDK4 in neuroblastoma tumors shows that CDK4 expression in neuroblastoma cell lines is comparable with tumors with high expression (Fig. 1*C*). The tumor panel has one sample and the cell line panel has two samples with extremely high expression of CDK4. We therefore screened the tumor and cell line panel for potential genomic amplification of CDK4. The tumor and cell lines with extremely high CDK4 expression are the tumors showing amplification of CDK4 (data not shown). The CDK4 expression shows a correlation with INSS tumor stage, loss of heterozygosity (LOH) of 1p, MYCN amplification, and, most significantly, survival as indicated by the Kaplan Meier curve (log-rank probability of 6.2×10^{-10}). The correlation to survival is also significantly independent of histologic classification (log-rank probability of 3.0×10^{-7} in neuroblastoma only) or MYCN amplification (log-rank probability of 5.0×10^{-5} in non–N-Myc amplified neuroblastoma only). CDK6 shows a similar pattern to Cyclin D1 (Fig. 1*D*) with a very significant correlation with the histologic classification of neuroblastic tumors (ganglioneuroma versus neuroblastoma unpaired Student's t test, $P = 8.0 \times 10^{-17}$).

High Cyclin D1 expression is restricted to neuroblasts. The difference in Cyclin D1 expression in ganglioneuroma and neuroblastoma, found in Affymetrix expression profiles, could be the result of the influx of Schwann cells in the tumor and dilution of a

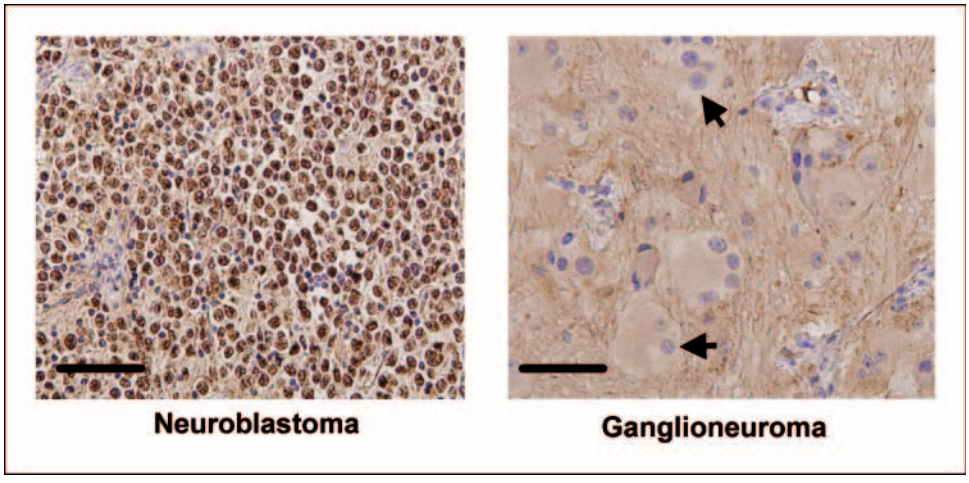

Figure 2. Immunohistochemical staining of a neuroblastoma and a ganglioneuroma tumor with an antibody against Cyclin D1. *Arrows,* two negative nuclei of ganglion cells; *scale bar,* 50 μm.

possible Cyclin D1 signal. Therefore, we stained paraffin-embedded tumor sections from 63 neuroblastomas, 26 ganglioneuroblastomas, and 8 ganglioneuromas with a Cyclin D1 antibody. Tissue was considered positive if at least 10% of the tumor cells showed specific nuclear staining, strongly positive when in at least 20% of the stained nuclei the hematoxylin counter stain was not visible any more, and focal-positive when only a part of the tumor showed nuclear staining. For 24 tumors, both Affymetrix and protein data were available. There was a clear correlation between the Cyclin D1 mRNA expression by microarray and the protein expression data by immunohistochemistry (data not shown). In the complete panel of 97 tumor samples that were analyzed for Cyclin D1 expression

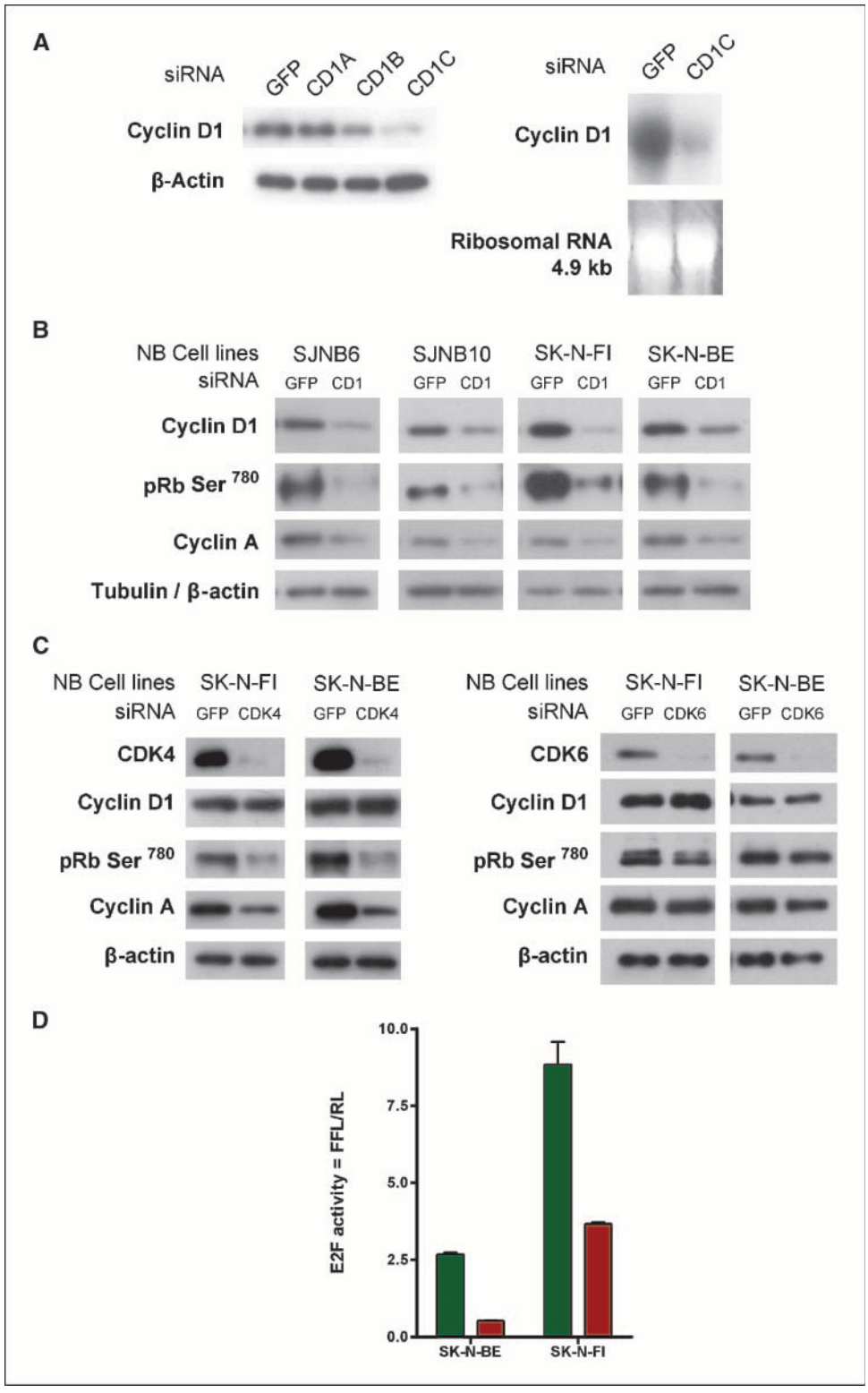

Figure 3. Cyclin D1 and CDK4 silencing in neuroblastoma cell lines causes pRb pathway inhibition. *A, left,* Western blot from SK-N-BE cell lysates 48 h after treatment with three different Cyclin D1 siRNAs and a GFP siRNA as negative control. The Western blot is incubated with a Cyclin D1 antibody and a β-actin antibody for loading control. *Right,* Northern blot from SK-N-BE cell lines 48 h after treatment with Cyclin D1 and GFP siRNA. The ethidium bromide staining of the rRNA 4.9-kb band is shown as loading control. *B,* Western blot from cell lysates of SJNB-6, SJNB-10, SK-N-FI, and SK-N-BE 48 h after treatment with Cyclin D1 (*CD1*) or GFP siRNA. Western blots were incubated with a Cyclin D1 antibody, an antibody specific for CDK4 phosphorylated pRb (pRb Ser^{780}), and a Cyclin A antibody. The Western blot was incubated with β-actin antibody for loading control. Because SJNB-6 has low β-actin expression, we used tubulin as loading control. *C,* Western blots from cell lysates of SK-N-FI and SK-N-BE 48 h after treatment with CDK4, CDK6, or GFP siRNA. Western blots were incubated with a CDK4 or CDK6 antibody, a Cyclin D1 antibody, an antibody specific for CDK4/CDK6 phosphorylated pRb (pRb Ser^{780}), and a Cyclin A antibody. The Western blot was incubated with β-actin antibody as loading control. *D,* E2F transcriptional activity 24 h after transfection with Cyclin D1 (*red*) or GFP (*green*) siRNA of neuroblastoma cell lines SK-N-BE and the SK-N-FI. E2F activity is shown as the firefly luciferase activity from the E2F-FF reporter construct divided by the Renilla luciferase activity from the cotransfected constitutionally active CMV-RL vector. These are the results of three independent experiments. *Error bars,* SD.

by immunohistochemistry, there was a clear correlation between the histologic classification and the Cyclin D1 expression levels (Table 1). In ganglioneuroma, not only the Schwannian stroma cells have low expression of Cyclin D1 but also the ganglion cells have low expression of Cyclin D1 compared with neuroblasts (Fig. 2). High Cyclin D1 expression that does not leave any hematoxylin visible is restricted to neuroblasts. These results indicate that Cyclin D1 might play a role in maintaining the undifferentiated phenotype of neuroblasts.

Cyclin D1 and CDK4 RNA interference causes pRb pathway inhibition. To study the functional relevance of Cyclin D1 and its kinase partners CDK4 and CDK6 in neuroblastoma, we used RNA interference to silence these genes in neuroblastoma cell lines. We first tested Cyclin D1 siRNAs in the neuroblastoma cell line SK-N-BE, which has a very high expression of Cyclin D1. As a negative control, we used an siRNA targeting the coding region of GFP. From three different siRNAs targeting the coding region of Cyclin D1, the CD1C siRNA showed the best reduction of Cyclin D1 mRNA and protein (85%; Fig. 3*A*). From our panel of neuroblastoma cell lines, we selected three more cell lines with high expression of Cyclin D1. Transfection of the Cyclin D1 siRNA (CD1-C) in SJ-NB 6, SJ-NB 10, and SK-N-FI showed a 70%, 43%, and 89% reduction of Cyclin D1, respectively (Fig. 3*B*). The silencing of the Cyclin D1 gene lasted for 4 days. To determine whether silencing of Cyclin D1 causes an effect on the downstream pRb pathway, we used a phosphospecific antibody against CDK4/CDK6 phosphorylated pRb (Ser^{780}). All four neuroblastoma cell lines transfected with the Cyclin D1 siRNA showed a decrease in Ser^{780} phosphorylated pRb (Fig. 3*B*). Hypophosphorylation of pRb causes inhibition of the E2F transcriptional activity. To show that the E2F transcriptional activity was indeed inhibited by the Cyclin D1 protein knockdown, we used a dual luciferase assay with a reporter construct containing six E2F binding sites. In the two tested neuroblastoma cell lines, SK-N-BE and SK-N-FI, a clear downregulation of E2F transcriptional activity was shown in the Cyclin D1 siRNA-treated cells compared with the GFP siRNA-treated cells

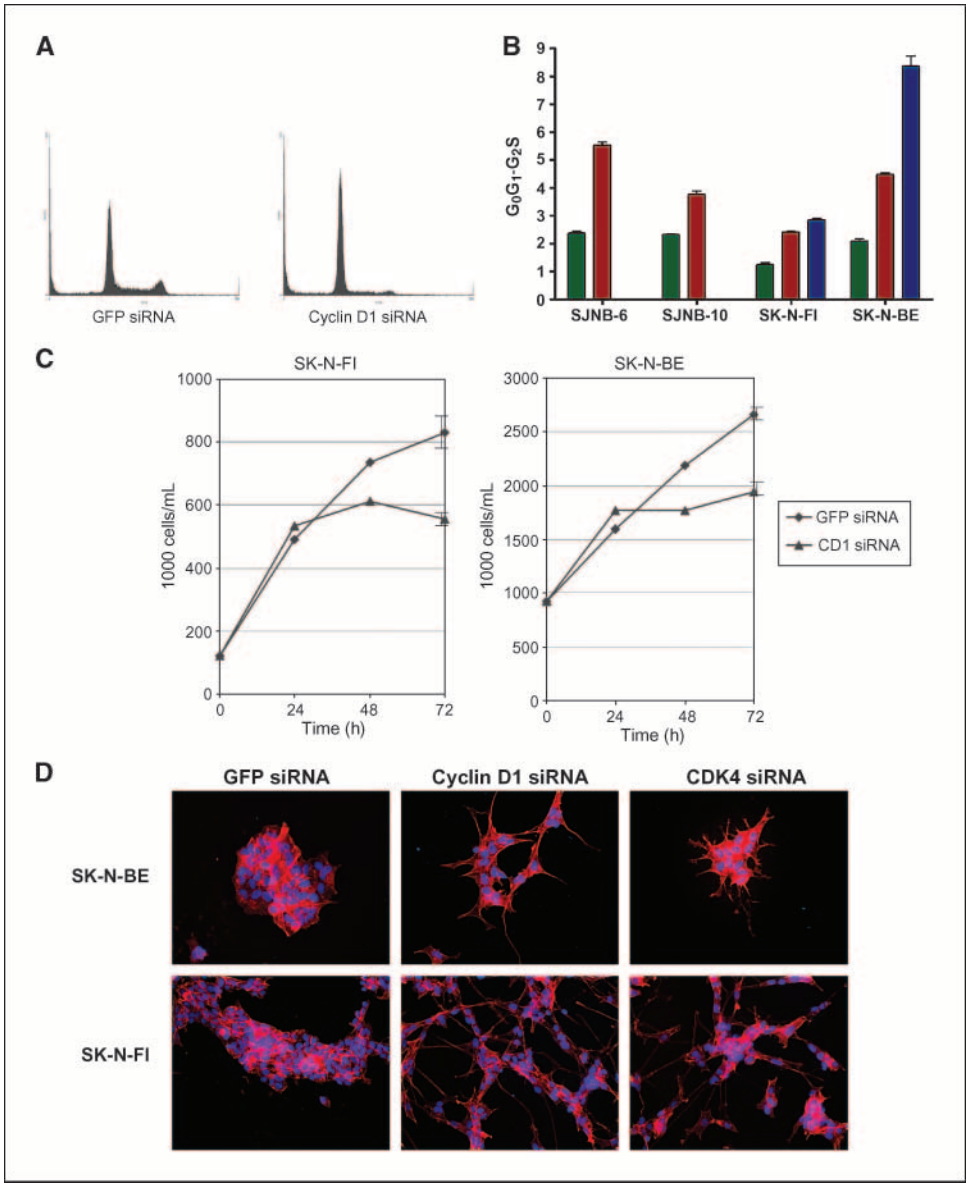

Figure 4. Phenotype analysis after Cyclin D1 and CDK4 silencing in neuroblastoma cell lines. *A,* FACS analysis of SK-N-BE nuclei 48 h after treatment with GFP and CD1 siRNA. *B,* bar plot of FACS analysis of the SJNB-6, SJNB-10, SK-N-BE, and SK-N-FI cell lines 48 h after transfection with GFP (*green*), Cyclin D1 (*red*), or CDK4 (*blue*) siRNA. The number of cells in G_1 and G_0 phase divided by the number of cells in G_2 and S phase. These are the results of four independent experiments. *Error bars,* SD. *C,* growth assays of SK-N-BE and SK-N-FI cell lines treated with Cyclin D1 and GFP siRNA. Cells were counted twice by Coulter counter in two separate experiments at 0, 24, 48, and 72 h. *Error bars,* SD. *D,* fluorescent microscopy of neuroblastoma cell lines SK-N-BE and SK-N-FI 72 h after treatment with GFP, Cyclin D1, or CDK4 siRNA. Cells were grown on glass. The actin fibers were stained with TRITC-labeled phalloidin and the nuclei with propidium iodide.

(Fig. 3*D*). E2F induces transcription of Cyclin A. Figure 3*B* shows that Cyclin A levels also decrease after Cyclin D1 silencing. To determine if silencing of the Cyclin D1 kinase partners results in the same downstream pathway effect, we also developed an effective CDK4 and CDK6 siRNA and transiently transfected the cell lines SK-N-BE and SK-N-FI. Western blot results show an effective knockdown of CDK4 in SK-N-BE and SK-N-FI 72 hours after transfection (Fig. 3*C*). The CDK4 silencing has no effect on Cyclin D1 protein levels. CDK4 silencing results in evident decrease in pRb phosphorylation and reduction of the E2F target protein Cyclin A. Also CDK6 was very efficiently silenced. However, CDK6 silencing hardly affected the Rb phosphorylation level, and also Cyclin A levels were not or hardly reduced (Fig. 3*C*). We conclude that knockdown of Cyclin D1 or its kinase partner CDK4 causes inhibition of the pRb-E2F pathway in neuroblastoma cell lines. CDK6 silencing hardly affects the pRb-E2F pathway.

G_1 cell cycle arrest and inhibition of cell growth after Cyclin D1 or CDK4 inhibition. The inhibition of the Cyclin D1-pRb-E2F pathway resulted in marked phenotypical effects in neuroblastoma cell lines. We performed fluorescence-activated cell sorting (FACS) analysis to evaluate the effect of Cyclin D1 inhibition on the cell cycle. The SK-N-FI, SK-N-BE, SJNB-6, and SJNB-10 cell lines were transfected with siRNA-targeting Cyclin D1 and GFP and harvested for FACS analysis after 48 hours. SK-N-BE shows a clear increase in G_0G_1 fraction and a decrease in G_2S fraction in the Cyclin D1 siRNA treatment compared with the GFP negative control (Fig. 4*A*). This results in a strong increase of the G_0G_1-G_2S ratio, which was also observed in the three other neuroblastoma cell lines tested (Fig. 4*B*). Also CDK4 inhibition by siRNA showed a strong G_1 arrest. In SK-N-BE, CDK4 silencing caused an even stronger G_1 arrest compared with Cyclin D1 silencing. This is probably due to a more effective knockdown. To analyze whether the G_1 cell cycle arrest results in growth inhibition, we performed growth assays in the SK-N-BE and SK-N-FI cell lines after Cyclin D1 silencing. Cells were trypsinized after 0, 24, 48, and 72 hours and counted with a Coulter counter. At the first 24 hours, no effect is seen on cell growth. At 48 and 72 hours, a significant cell growth reduction is seen in the two cell lines transfected with Cyclin D1 siRNA cells compared with the control cells (Fig. 4*C*). The silencing of CDK6 did not result in growth inhibition (data not shown).

Cyclin D1 and CDK4 silencing induces neuronal differentiation. The growth inhibition observed in Cyclin D1 siRNA-treated cells can be caused by a growth arrest or cell death. In Cyclin D1 siRNA-treated neuroblastoma cell lines, we did not observe an increased number of detached cells suggesting that no increase in apoptosis has occurred. FACS analysis did not show an increase of the sub-G_1 fraction at 48 and 72 hours after transfection of Cyclin D1 or CDK4 siRNA in cell lines SK-N-BE, SK-N-FI, SJNB-6, and SJNB-10. Also a TUNEL assay performed at 48 hours after Cyclin D1 knockdown showed no increase in the apoptotic index in any of the cell lines. However, analysis of neuroblastoma cells after Cyclin D1 or CDK4 silencing revealed a strong phenotype. Silencing of CDK6 did not induce this differentiated phenotype (data not shown). Cyclin D1 and CDK4 siRNA-treated neuroblastoma cells showed an extensive increase in the number of neurite extensions per cell and the length of those extensions compared with the negative control. In Fig. 4*D*, this neuronal differentiation is visualized by staining actin with TRITC-labeled phalloidin. This suggests that neuroblasts differentiate toward a neuronal phenotype after inhibition of the G_1 checkpoint.

Cyclin D1 and CDK4 silencing induces a neuronal differentiation pattern on mRNA profiling. To further analyze the characteristics of the differentiation pattern after Cyclin D1 or CDK4 silencing, we performed Affymetrix expression profiling. The SK-N-BE cell line was transfected with Cyclin D1 siRNA, CDK4 siRNA, and GFP siRNA as control. RNA was isolated at time point 0 and 48 hours after siRNA transfection and hybridized on Affymetrix HG-U133-plus2 microarrays. All assays were performed in triplo, and results were analyzed on MAS5 normalized data. Firstly, we excluded all genes without a present call based on the MAS5 algorithm. Secondly, we excluded all genes that were significantly regulated (unpaired *t* test, $P < 0.01$) between time points 0 and 48 hours in the GFP transfected cells to avoid selection of genes that are also regulated due to transfection procedures. We subsequently selected genes that were at least 2-fold and significantly (unpaired *t* test, $P < 0.01$) regulated both in the Cyclin D1 and CDK4 silenced cells compared with GFP siRNA-treated cells 48 hours after transfection. This resulted in a set of 129 regulated genes, of which 70 were up-regulated and 59 were down-regulated. These genes were grouped according to their function derived from the NCI Gene and OMIM databases (Table 2*A* and *B*). For 38 of the up-regulated genes, a functional description was given, and 11 of those genes are involved in neuronal processes as neuronal development, signaling, or neurotransmitter secretion. This indicates that these cells show a change in expression pattern toward a neuronal phenotype which reflects our observations. The majority of down-regulated genes are involved in cell cycle regulation or transcriptional regulation. The genes marked with an asterisk are well-established E2F target genes (23–27), which confirms the reliability of our results, because the Cyclin D1/CDK4 complex functions through phosphorylation of pRb and activation of the E2F transcription factor.

Discussion

We report a very high mRNA expression of Cyclin D1 in neuroblastoma compared with all other normal tissue libraries and tumor libraries, including tumor libraries with known high frequencies of Cyclin D1 genetic aberrations. The protein expression correlates well with the mRNA expression levels, and Cyclin D1 is mainly located in the nucleus of malignant neuroblasts. CDK4 and CDK6, the kinase partners of Cyclin D1, are also highly expressed and correlate with unfavorable prognosis and histologic classification, respectively. These findings strongly suggest a role for G_1 entry checkpoint dysregulation in the etiology of neuroblastoma. Silencing of Cyclin D1 and CDK4 clearly leads to inactivation of the pRb pathway and E2F transcription. For CDK6, the effect on the pRb pathway is less outspoken. Probably CDK4 plays a more pronounced role in neuroblastoma cell lines compared with CDK6. This does not exclude a role for CDK6 *in vivo*.

Apart from cell cycle regulation, these G_1 entry checkpoint regulators have been linked to other signal transduction routes. The apoptotic response which has been reported after Cyclin D1 silencing by other authors (28, 29) was not found after Cyclin D1 or CDK4 silencing in neuroblastoma as shown by FACS, TUNNEL assay, and microarray expression analysis. However, we report a change into a more differentiated phenotype after Cyclin D1 and CDK4 inhibition. The involvement of Cyclin D1 in neuronal differentiation processes has been suggested previously (12, 30, 31). In neuroblastoma, several authors linked Cyclin D1 nuclear overexpression to neuronal differentiation, but only as a downstream

Table 2. Up-regulated and down-regulated genes after Cyclin D1 and CDK4 silencing

Probeset ID	HUGO ID	Fold regulation		Gene name	Gene function
		CD1 siRNA	CDK4 siRNA		
A. Up-regulated genes					
Neuronal Processes					
205373_at	*CTNNA2*	4.2	4.0	*Catenin (cadherin-associated protein), α2*	Neuronal development
210341_at	*MYT1*	3.8	3.0	*Myelin transcription factor 1*	Neuronal development
206408_at	*LRRTM2*	3.1	3.7	*Leucine rich repeat transmembrane neuronal 2*	Neuronal development
214761_at	*ZNF423*	2.4	2.1	*Zinc finger protein 423*	Neuronal development
239293_at	*NRSN1*	2.1	2.1	*Neurensin 1*	Neuronal development
203889_at	*SCG5*	3.3	3.6	*Secretogranin V (7B2 protein)*	Neuropeptide signaling
224625_x_at	*SERF2*	2.2	2.9	*Small EDRK-rich factor 2*	Neuropeptide signaling
225093_at	*UTRN*	3.0	5.1	*Utrophin (homologous to dystrophin)*	Neurotransmitter secretion
219578_s_at	*CPEB1*	3.0	2.3	*Cytoplasmic polyadenylation element binding protein 1*	Neurotransmitter secretion
209737_at	*MAGI2*	2.2	4.3	*Membrane associated guanylate kinase 2*	Neurotransmitter secretion
241957_x_at	*LIN7B*	2.1	2.9	*Lin-7 homologue B*	Neurotransmitter secretion
Development and differentiation					
203939_at	*NT5E*	5.9	10.6	*5′-Nucleotidase, ecto (CD73)*	Development
203408_s_at	*SATB1*	3.5	3.2	*Special AT-rich sequence binding protein 1*	Development
231943_at	*ZFP28*	2.3	2.8	*Zinc finger protein 28 homologue (mouse)*	Development
203706_s_at	*FZD7*	2.2	6.4	*Frizzled homologue 7 (Drosophila)*	Development
242794_at	*MAML3*	2.1	2.1	*Mastermind-like 3 (Drosophila)*	Development
Cell cycle					
225912_at	*TP53INP1*	14.1	3.0	*Tumor protein p53 inducible nuclear protein 1*	Cell cycle (inhibition)
212593_s_at	*PDCD4*	4.1	5.9	*Programmed cell death 4 (neoplastic transformation inhibitor)*	Cell cycle (inhibition)
Transcription and translation					
238447_at	*RBMS3*	2.8	2.2	*RNA binding motif, single stranded interacting protein*	mRNA processing
235296_at	*EIF5A2*	2.6	2.3	*Eukaryotic translation initiation factor 5A2*	mRNA processing
238549_at	*CBFA2T2*	2.7	2.1	*Core-binding factor α subunit 2; translocated to 2*	Transcription
Other or unknown					
210130_s_at	*TM7SF2*	9.1	6.4	*Transmembrane 7 superfamily member 2*	Cholesterol metabolism
226390_at	*STARD4*	5.8	2.7	*START domain containing 4, sterol regulated*	Cholesterol metabolism
202708_s_at	*HIST2H2BE*	6.3	11.6	*Histone 2, H2be*	Histone
232035_at	*HIST1H4H*	6.0	12.5	*Histone 1, H4h*	Histone
225245_x_at	*H2AFJ*	2.7	4.6	*H2A histone family, member J*	Histone
205719_s_at	*PAH*	6.9	5.6	*Phenylalanine hydroxylase*	Phenylalanine catabolism
201061_s_at	*STOM*	4.4	4.0	*Stomatin*	Cytoskeleton organization
202992_at	*C7*	4.0	3.3	*Complement component 7*	Complement activation
218341_at	*PPCS*	3.5	4.2	*Phosphopantothenoylcysteine synthetase*	CoA biosynthesis
221471_at	*SERINC3*	3.4	3.6	*Serine incorporator 3*	Apoptosis inhibition
202388_at	*RGS2*	3.2	4.0	*Regulator of G-protein signaling 2, 24 kDa*	Ca(2+) signaling
201172_x_at	*ATP6V0E*	3.0	2.7	*ATPase, H+ transporting, lysosomal 9 kDa, V0 subunit e*	Ion transport
209392_at	*ENPP2*	2.8	2.2	*Ectonucleotide pyrophosphatase/phosphodiesterase 2*	Chemotaxis
1554741_s_at	*FGF7*	2.6	3.3	*Fibroblast growth factor 7*	Growth factor
209751_s_at	*TRAPPC2*	2.2	2.3	*Trafficking protein particle complex 2*	ER to Golgi transport
202119_s_at	*CPNE3*	2.1	2.3	*Copine III*	Phospholipid-binding
219315_s_at	*C16ORF30*	2.1	2.2	*chromosome 16 open reading frame 30*	Cell adhesion
225325_at	*FLJ20160*	10.2	4.6	*FLJ20160 protein*	Unknown
219543_at	*MAWBP*	4.5	3.4	*Phenazine biosynthesis-like protein domain containing*	Unknown
221467_at	*MC4R*	4.5	10.2	*Melanocortin 4 receptor*	Unknown
1552733_at	*KLHDC1*	4.3	4.4	*Kelch domain containing 1*	Unknown
235953_at	*ZNF610*	3.7	6.5	*Zinc finger protein 610*	Unknown
1557137_at	*TMEM17*	3.6	3.3	*Transmembrane protein 17*	Unknown
226158_at	*KLHL24*	3.4	3.0	*Kelch-like 24 (Drosophila)*	Unknown
240592_at	*LCORL*	3.1	4.0	*Ligand-dependent nuclear receptor corepressor-like*	Unknown
226104_at	*RNF170*	3.1	5.7	*Ring finger protein 170*	Unknown
225397_at	*CCDC32*	3.0	3.6	*Coiled-coil domain containing 32*	Unknown
227181_at	*LOC348801*	2.8	2.2	*Hypothetical protein LOC348801*	Unknown

(*Continued on the following page*)

Table 2. Up-regulated and down-regulated genes after Cyclin D1 and CDK4 silencing (Cont'd)

Probeset ID	HUGO ID	Fold regulation		Gene name	Gene function
		CD1 siRNA	CDK4 siRNA		
224981_at	*LOC124446*	2.7	2.3	*Hypothetical protein BC017488*	Unknown
219013_at	*GALNT11*	2.7	3.5	*Galactosamine N-acetylgalactosaminyltransferase 11*	Unknown
226583_at	*FLJ40142*	2.6	2.4	*FLJ40142 protein*	Unknown
219348_at	*MDS032*	2.5	2.7	*MDS032*	Unknown
1553099_at	*TIGD1*	2.4	2.5	*Tigger transposable element derived 1*	Unknown
229491_at	*LOC133308*	2.3	2.9	*Hypothetical protein BC009732*	Unknown
225446_at	*BRWD1*	2.3	3.2	*Bromodomain and WD repeat domain containing 1*	Unknown
235174_s_at	*LOC641917*	2.3	5.4	*Hypothetical protein LOC641917*	Unknown
1556180_at	*LOC255458*	2.2	3.9	*Hypothetical protein LOC255458*	Unknown
226126_at	*MGC16169*	2.2	2.1	*Hypothetical protein MGC16169*	Unknown
41387_r_at	*JMJD3*	2.1	2.6	*Jumonji domain containing 3*	Unknown
226235_at	*LOC339290*	2.1	2.3	*Hypothetical protein LOC339290*	Unknown
226575_at	*ZNF462*	2.1	3.2	*Zinc finger protein 462*	Unknown
224443_at	*C1ORF97*	2.1	3.7	*Chromosome 1 open reading frame 97*	Unknown
218694_at	*ARMCX1*	2.1	2.5	*Armadillo repeat containing, X-linked 1*	Unknown
221845_s_at	*CLPB*	2.1	2.8	*ClpB caseinolytic peptidase B homologue (E. coli)*	Unknown
213939_s_at	*RUFY3*	2.0	2.3	*RUN and FYVE domain containing 3*	Unknown
78495_at	*DKFZP762P2111*	2.0	3.3	*Hypothetical protein DKFZp762P2111*	Unknown
230298_at	*LOC153364*	2.0	3.1	*Similar to metallo-β-lactamase superfamily protein*	Unknown
222931_s_at	*THNSL1*	2.0	4.5	*Threonine synthase-like 1 (bacterial)*	Unknown
B. Down-regulated genes					
Cell cycle					
203967_at	*CDC6**	−3.4	−4.4	*CDC6 cell division cycle 6 homologue*	Cell cycle (progression)
228033_at	*E2F7**	−2.5	−5.4	*E2F transcription factor 7*	Cell cycle (progression)
213906_at	*MYBL1**	−2.4	−4.8	*Myeloblastosis viral oncogene homologue like 1*	Cell cycle (progression)
204825_at	*MELK**	−2.2	−4.6	*Maternal embryonic leucine zipper kinase*	Cell cycle (progression)
224428_s_at	*CDCA7**	−2.0	−2.2	*Cell division cycle associated 7*	Cell cycle (progression)
204159_at	*CDKN2C**	−2.4	−3.1	*Cyclin-dependent kinase inhibitor 2C*	Cell cycle (inhibition)
205235_s_at	*MPHOSPH1*	−3.4	−5.3	*M-phase phosphoprotein 1*	Mitosis
218542_at	*CEP55*	−3.2	−5.5	*Centrosomal protein 55 kDa*	Mitosis
221520_s_at	*CDCA8*	−3.0	−8.4	*Cell division cycle associated 8*	Mitosis
218355_at	*KIF4A**	−2.8	−5.5	*Kinesin family member 4A*	Mitosis
204444_at	*KIF11*	−2.6	−4.7	*Kinesin family member 11*	Mitosis
222848_at	*CENPK*	−2.4	−5.9	*Centromere protein K*	Mitosis
228323_at	*CASC5*	−2.4	−4.8	*Cancer susceptibility candidate 5*	Mitosis
210052_s_at	*TPX2*	−2.4	−4.8	*TPX2, microtubule-associated, homologue*	Mitosis
208079_s_at	*AURKA*	−2.4	−4.5	*Aurora kinase A*	Mitosis
209408_at	*KIF2C*	−2.3	−3.5	*Kinesin family member 2C*	Mitosis
226661_at	*CDCA2*	−2.3	−5.0	*Cell division cycle associated 2*	Mitosis
212949_at	*BRRN1*	−2.3	−4.9	*Barren homologue 1 (Drosophila)*	Mitosis
209891_at	*SPBC25*	−2.1	−6.5	*Spindle pole body component 25 homologue*	Mitosis
231772_x_at	*CENPH*	−2.1	−3.9	*Centromere protein H*	Mitosis
207828_s_at	*CENPF*	−2.1	−3.7	*Centromere protein F, 350/400ka (mitosin)*	Mitosis
218755_at	*KIF20A*	−2.0	−4.4	*Kinesin family member 20A*	Mitosis
219703_at	*MNS1**	−3.2	−4.0	*Meiosis-specific nuclear structural 1*	Meiosis
213951_s_at	*PSMC3IP*	−2.4	−4.0	*PSMC3 interacting protein*	Meiosis
210983_s_at	*MCM7**	−2.8	−4.0	*Minichromosome maintenance deficient 7*	DNA replication
204126_s_at	*CDC45L*	−2.3	−4.9	*CDC45 cell division cycle 45-like*	DNA replication
203209_at	*RFC5*	−2.1	−3.5	*Replication factor C (activator 1) 5*	DNA replication
Transcription and translation					
229551_x_at	*ZNF367*	−3.5	−9.0	*Zinc finger protein 367*	Transcription
227787_s_at	*THRAP6*	−2.5	−3.2	*Thyroid hormone receptor associated protein 6*	Transcription
204033_at	*TRIP13*	−2.4	−2.5	*Thyroid hormone receptor interactor 13*	Transcription
225081_s_at	*CDCA7L*	−2.3	−5.8	*Cell division cycle associated 7-like*	Transcription

(*Continued on the following page*)

Table 2. Up-regulated and down-regulated genes after Cyclin D1 and CDK4 silencing (Cont'd)

Probeset ID	HUGO ID	Fold regulation		Gene name	Gene function
		CD1 siRNA	CDK4 siRNA		
201726_at	*ELAVL1*	−2.2	−2.5	*Embryonic lethal, abnormal vision-like 1*	mRNA processing
Development and differentiation					
224675_at	*MESDC2*	−3.5	−2.4	*Mesoderm development candidate 2*	Development
218459_at	*TOR3A*	−2.5	−2.2	*Torsin family 3, member A*	Development
224617_at	*ROD1*	−3.4	−6.0	*ROD1 regulator of differentiation 1*	Differentiation
218585_s_at	*DTL*	−3.3	−5.0	*Denticleless homologue*	Differentiation
Other or Unknown					
209621_s_at	*PDLIM3*	−3.0	−2.4	*PDZ and LIM domain 3*	Cytoskeleton org.
213511_s_at	*MTMR1*	−2.6	−2.8	*Myotubularin related protein 1*	Cytoskeleton org.
212836_at	*POLD3*	−2.6	−4.8	*Polymerase δ 3, accessory subunit*	DNA repair
227059_at	*GPC6*	−2.2	−4.8	*Glypican 6*	Cell growth
39248_at	*AQP3*	−2.1	−2.8	*Aquaporin 3 (gill blood group)*	Water channel
212573_at	*ENDOD1*	−3.5	−3.4	*Endonuclease domain containing 1*	Unknown
228728_at	*FLJ21986*	−2.9	−2.6	*Hypothetical protein FLJ21986*	Unknown
228281_at	*FLJ25416*	−2.7	−5.2	*Hypothetical protein FLJ25416*	Unknown
226416_at	*THEX1*	−2.6	−2.8	*Three prime histone mRNA exonuclease 1*	Unknown
223215_s_at	*C14ORF100*	−2.5	−2.5	*Chromosome 14 open reading frame 100*	Unknown
205347_s_at	*TMSL8*	−2.5	−6.5	*Thymosin-like 8*	Unknown
238756_at	*GAS2L3*	−2.5	−4.4	*Growth arrest-specific 2 like 3*	Unknown
222617_s_at	*C10ORF84*	−2.3	−2.1	*Chromosome 10 open reading frame 84*	Unknown
225687_at	*FAM83D*	−2.2	−2.0	*Family with sequence similarity 83, member D*	Unknown
218726_at	*DKFZP762E131*	−2.2	−4.9	*Hypothetical protein DKFZp762E1312*	Unknown
228559_at	*C16ORF60*	−2.2	−3.3	*Centromere protein N*	Unknown
223606_x_at	*KIAA1704*	−2.2	−2.7	*KIAA1704*	Unknown
241838_at	*LOC644112*	−2.1	−3.7	*Similar to splicing factor 3b, subunit 4*	Unknown
219038_at	*MORC4*	−2.1	−5.7	*MORC family CW-type zinc finger 4*	Unknown
231855_at	*KIAA1524*	−2.1	−4.5	*KIAA1524*	Unknown
202503_s_at	*KIAA0101*	−2.1	−3.4	*KIAA0101*	Unknown
228069_at	*FAM54A*	−2.1	−4.1	*Family with sequence similarity 54, member A*	Unknown
221677_s_at	*DONSON*	−2.0	−3.5	*Downstream neighbor of SON*	Unknown

NOTE: The algorithm is discussed in detail in Results. The table gives the probesets that represent the gene (see Materials and Methods for probeset selection), the HUGO identifier for the regulated gene, the fold regulation after cyclin D1 and CDK4 silencing, the gene name, and the gene function which was taken from the NCI gene database (http://www.ncbi.nlm.nih.gov/entrez/query.fcgi?db=gene) and the OMIM database (http://www.ncbi.nlm.nih.gov/entrez/query.fcgi?db=OMIM). An asterisk indicates that a gene is an E2F target gene. References are given in Results.

effect of other regulating genes (14, 15). We now show that Cyclin D1 overexpression itself is a driving event that prevents differentiation in neuroblastoma. First, we show a very high expression of Cyclin D1 in neuroblasts and low Cyclin D1 levels in differentiated ganglion cells *in vivo*. *In vitro* we show neuronal outgrowth after Cyclin D1 or CDK4 silencing and induction of a neuronal expression signature by Affymetrix microarray analysis. This is not in contrast with the findings that growth signaling pathways determine differentiation patterns in nonmalignant neuroblasts and influence the differentiation state of neuroblastoma. These signal transduction routes most frequently involve the transcriptional regulation of Cyclin D1, and thus, the effect on neuronal differentiation by these signal transduction routes could partly function through Cyclin D1 regulation (32).

The signal transduction routes that cause the distinct phenotypical effects (cell cycle arrest and neuronal differentiation) on neuroblastoma could both involve E2F activity. Many of the cell cycle progression genes that show up in the microarray profile are E2F target genes. The down-regulation of the cell cycle inhibitor CDKN2C seems in conflict with the cell cycle arrest, but again, this gene is an established E2F target. The phenotypic effect of neuronal differentiation could involve the strongly regulated MELK, which is an established E2F target and a crucial player in maintaining an undifferentiated phenotype in neuronal progenitor cells (27, 33, 34). In our neuroblastoma panel, the Affymetrix expression of MELK is strongly correlated to histologic classification and prognosis (data not shown). Further studies have to identify the exact role of this gene in the pathogenesis of neuroblastoma. The expression profiling after Cyclin D1 and CDK4 silencing also allows us to identify new downstream players involved in neuronal differentiation in neuroblastoma. Zfp423 is a newly identified transcription factor controlling proliferation and differentiation of neural precursors in cerebellar vermis formation. MYT1 is a transcription factor that has a role in the regeneration of oligodendrocyte lineage cells in response to demyelination (35, 36).

We conclude that the high-expression Cyclin D1 and CDK4 that correlates with histologic subtypes and prognosis together

with the previous reported genetic aberrations indicate that these G_1-regulating genes are crucial players in neuroblastoma tumorigenesis. The resulting E2F transcriptional activity seems to regulate cell cycle, as well as neuronal differentiation signal transduction.

Acknowledgments

Received 8/24/2007; revised 1/18/2008; accepted 2/21/2008.

The costs of publication of this article were defrayed in part by the payment of page charges. This article must therefore be hereby marked *advertisement* in accordance with 18 U.S.C. Section 1734 solely to indicate this fact.

References

1. Ambros IM, Hata J, Joshi VV, et al. Morphologic features of neuroblastoma (Schwannian stroma-poor tumors) in clinically favorable and unfavorable groups. Cancer 2002;94:1574–83.

2. Shimada H, Ambros IM, Dehner LP, et al. The International Neuroblastoma Pathology Classification (the Shimada system). Cancer 1999;86:364–72.

3. Ciccarone V, Spengler BA, Meyers MB, Biedler JL, Ross RA. Phenotypic diversification in human neuroblastoma cells: expression of distinct neural crest lineages. Cancer Res 1989;49:219–25.

4. Hoehner JC, Gestblom C, Hedborg F, Sandstedt B, Olsen L, Pahlman S. A developmental model of neuroblastoma: differentiating stroma-poor tumors' progress along an extra-adrenal chromaffin lineage. Lab Invest 1996;75:659–75.

5. Hoehner JC, Hedborg F, Eriksson L, et al. Developmental gene expression of sympathetic nervous system tumors reflects their histogenesis. Lab Invest 1998;78:29–45.

6. Ambros IM, Zellner A, Stock C, Amann G, Gadner H, Ambros PF. Proof of the reactive nature of the Schwann cell in neuroblastoma and its clinical implications. Prog Clin Biol Res 1994;385:331–7.

7. Ambros IM, Amann G, Ambros PF. Correspondence re: J. Mora, et al., Neuroblastic and Schwannian stromal cells of neuroblastoma are derived from a tumoral progenitor cell. Cancer Res 2002;62:2986–7.

8. Mora J, Cheung NK, Juan G, et al. Neuroblastic and Schwannian stromal cells of neuroblastoma are derived from a tumoral progenitor cell. Cancer Res 2001;61:6892–8.

9. Bibel M, Barde YA. Neurotrophins: key regulators of cell fate and cell shape in the vertebrate nervous system. Genes Dev 2000;14:2919–37.

10. Matsumoto K, Wada RK, Yamashiro JM, Kaplan DR, Thiele CJ. Expression of brain-derived neurotrophic factor and p145TrkB affects survival, differentiation, and invasiveness of human neuroblastoma cells. Cancer Res 1995;55:1798–806.

11. Nakagawara A, rima-Nakagawara M, Scavarda NJ, Azar CG, Cantor AB, Brodeur GM. Association between high levels of expression of the TRK gene and favorable outcome in human neuroblastoma. N Engl J Med 1993;328:847–54.

12. McClellan KA, Slack RS. Novel functions for cell cycle genes in nervous system development. Cell Cycle 2006;5:1506–13.

13. Cesi V, Tanno B, Vitali R, et al. Cyclin D1-dependent regulation of B-myb activity in early stages of neuroblastoma differentiation. Cell Death Differ 2002;9:1232–9.

14. Georgopoulou N, Hurel C, Politis PK, Gaitanou M, Matsas R, Thomaidou D. BM88 is a dual function molecule inducing cell cycle exit and neuronal differentiation of neuroblastoma cells via Cyclin D1 down-regulation and retinoblastoma protein hypophosphorylation. J Biol Chem 2006;281:33606–20.

15. Sumrejkanchanakij P, Eto K, Ikeda MA. Cytoplasmic sequestration of Cyclin D1 associated with cell cycle withdrawal of neuroblastoma cells. Biochem Biophys Res Commun 2006;340:302–8.

16. Sherr CJ. Cancer cell cycles. Science 1996;274:1672–7.

17. Easton J, Wei T, Lahti JM, Kidd VJ. Disruption of the cyclin D/cyclin-dependent kinase/INK4/retinoblastoma protein regulatory pathway in human neuroblastoma. Cancer Res 1998;58:2624–32.

18. Heiskanen MA, Bittner ML, Chen Y, et al. Detection of gene amplification by genomic hybridization to cDNA microarrays. Cancer Res 2000;60:799–802.

19. Su WT, Alaminos M, Mora J, Cheung NK, La Quaglia MP, Gerald WL. Positional gene expression analysis identifies 12q overexpression and amplification in a subset of neuroblastomas. Cancer Genet Cytogenet 2004;154:131–7.

20. Molenaar JJ, van Sluis P, Boon K, Versteeg R, Caron HN. Rearrangements and increased expression of Cyclin D1 (CCND1) in neuroblastoma. Genes Chromosomes Cancer 2003;36:242–9.

21. Cheng NC, Beitsma M, Chan A, et al. Lack of class I HLA expression in neuroblastoma is associated with high N-myc expression and hypomethylation due to loss of the MEMO-1 locus. Oncogene 1996;13:1737–44.

22. Lukas J, Herzinger T, Hansen K, et al. Cyclin E-induced S phase without activation of the pRb/E2F pathway. Genes Dev 1997;11:1479–92.

23. Bracken AP, Ciro M, Cocito A, Helin K. E2F target genes: unraveling the biology. Trends Biochem Sci 2004;29:409–17.

24. Ishida S, Huang E, Zuzan H, et al. Role for E2F in control of both DNA replication and mitotic functions as revealed from DNA microarray analysis. Mol Cell Biol 2001;21:4684–99.

25. Vernell R, Helin K, Muller H. Identification of target genes of the p16INK4A-pRB-E2F pathway. J Biol Chem 2003;278:46124–37.

26. Di Stefano L, Jensen MR, Helin K. E2F7, a novel E2F featuring DP-independent repression of a subset of E2F-regulated genes. EMBO J 2003;22:6289–98.

27. Verlinden L, Eelen G, Beullens I, et al. Characterization of the condensin component Cnap1 and protein kinase Melk as novel E2F target genes down-regulated by 1,25-dihydroxyvitamin D3. J Biol Chem 2005;280:37319–30.

28. Sauter ER, Yeo UC, von Stemm A, et al. Cyclin D1 is a candidate oncogene in cutaneous melanoma. Cancer Res 2002;62:3200–6.

29. Sauter ER, Nesbit M, Litwin S, Klein-Szanto AJ, Cheffetz S, Herlyn M. Antisense Cyclin D1 induces apoptosis and tumor shrinkage in human squamous carcinomas. Cancer Res 1999;59:4876–81.

30. Sumrejkanchanakij P, Tamamori-Adachi M, Matsunaga Y, Eto K, Ikeda MA. Role of Cyclin D1 cytoplasmic sequestration in the survival of postmitotic neurons. Oncogene 2003;22:8723–30.

31. Spinella MJ, Freemantle SJ, Sekula D, Chang JH, Christie AJ, Dmitrovsky E. Retinoic acid promotes ubiquitination and proteolysis of Cyclin D1 during induced tumor cell differentiation. J Biol Chem 1999;274:22013–8.

32. Pestell RG, Albanese C, Reutens AT, Segall JE, Lee RJ, Arnold A. The cyclins and cyclin-dependent kinase inhibitors in hormonal regulation of proliferation and differentiation. Endocr Rev 1999;20:501–34.

33. Cordes S, Frank CA, Garriga G. The C. elegans MELK ortholog PIG-1 regulates cell size asymmetry and daughter cell fate in asymmetric neuroblast divisions. Development 2006;133:2747–56.

34. Nakano I, Paucar AA, Bajpai R, et al. Maternal embryonic leucine zipper kinase (MELK) regulates multipotent neural progenitor proliferation. J Cell Biol 2005;170:413–27.

35. Alcaraz WA, Gold DA, Raponi E, Gent PM, Concepcion D, Hamilton BA. Zfp423 controls proliferation and differentiation of neural precursors in cerebellar vermis formation. Proc Natl Acad Sci U S A 2006;103:19424–9.

36. Bellefroid EJ, Bourguignon C, Hollemann T, et al. X-MyT1, a *Xenopus* C2HC-type zinc finger protein with a regulatory function in neuronal differentiation. Cell 1996;87:1191–202.